using a peak detection or a thresholded centroid algorithm. Since peak localization schemes work well for point contacts, and centroid localization schemes work better for larger contact areas, algorithm selection should be based on manipulation object types. If this information is not available, a thresholded centroid algorithm should be a good compromise.

With care, both of these sensing schemes can provide contact localization accuracy of less than a millimeter in real manipulation tasks. This should be sufficient for a large number of application domains. Regarding the general question of which type of sensor should be used, or which sensor performs better, other benefits of each sensor should be considered as well. The force sensor has many other uses such as directly measuring contact forces and implementing stiffness controllers. The array sensor can provide shape information as well as pressure distribution of the contact area. Naturally, both sensors can be used to provide redundant information to increase robustness of the entire system.

Acknowledgments

The authors would like to thank Marc Tremblay, Dean Chang, and Jim Hyde of Stanford University for their help with the experimental component of this work, and Ron Fearing of the University of California at Berkeley for providing the array sensor electronics design. This work was supported by the Office of Naval Research under ONR Grants No. N00014-92-J-1814 and N00014-92-J-1887. Support for the first author was provided by a Doctoral Fellowship from Hughes Space and Communications Company.

References

A. D. Berger and P. K. Khosla. Using tactile data for real-time feedback. *International Journal of Robotics Research*, 10(2):88-102, April 1991.

A. Bicchi and G. Canepa. Optimal design of multivariate sensors. *Measurement Science & Technology,* 5(4):319-32, 1993

A. Bicchi, M. Bergamasco, P. Dario, and A. Fiorillo. Integrated tactile sensing for gripper fingers. *Proceedings of the 7th International Conference on Robot Vision and Sensory Controls,* Zurich, February 1988.

A. Bicchi, J. K. Salisbury, and D. L. Brock. Contact sensing from force measurements. *International Journal of Robotics Research*, 12(3):249-262, June 1993.

A. Bicchi. Intrinsic contact sensing for soft fingers. In *The Proceedings of the 1990 IEEE International Conference on Robotics and Automation*, pages 968-973, Cincinnati, OH, May 1990.

D. Brock and S. Chiu. Environment perception of an articulated robot hand using contact sensors. *Robotics and Manufacturing Automation,* volume PED 15, pages 89-96, ASME Winter Annual Meeting. Miami, November 1985.

Cole, A., P. Hsu, and S. Sastry, Dynamic control of sliding by robot hands for regrasping. *IEEE Transactions on Robotics and Automation,* 8(1):42-52, 1992.

M. R. Cutkosky and I. Kao. Computing and controlling compliance of a robotics hand. *IEEE Transactions on Robotics and Automation*, 5(2):151-165, April 1989.

R. S. Fearing. Tactile sensing mechanisms. *International Journal of Robotics Research*, 9(3):3–23, June 1990.

R. D. Howe, "Tactile sensing and control of robotic manipulation," *Journal of Advanced Robotics*, 8(3):245-261, 1994.

R. D. Howe and M. R. Cutkosky, Dynamic tactile sensing: Perception of fine surface features with stress rate sensing, *IEEE Transactions on Robotics and Automation*, 9(2):140-151, April 1993.

R. D. Howe, I. Kao, and M. R. Cutkosky. The sliding of robot fingers under torsion and shear loading, *Proceedings of the 1988 IEEE International Conference on Robotics and Automation*, pages 103-108, Philadelphia 1988.

I. Kao and M. R. Cutkosky. Quasistatic manipulation with compliance and sliding, *International Journal of Robotics Research,* 11(1):20-40, Feb. 1992.

J. Kerr and B. Roth. Analysis of multifingered hands. *The International Journal of Robotics Research*, 4(4):3-17, 1986.

Z. Li, P. Hsu, and S. Sastry. Grasping and coordinated manipulation by a multifingered robot hand. *International Journal of Robotics Research,* 8(2):33-50, August 1989.

H. Maekawa, K. Komoriya, and K. Tanie. Manipulation of an unknown object by multifingered hands with rolling contact using tactile feedback. *Proceedings of the 1992 IEEE/RSJ International Conference on Intelligent Robots and Systems, IROS '92*. pages 1877-1882, Raleigh, NC, July 7-10, 1992.

Montana, D.J., The kinematics of contact and grasp. *International Journal of Robotics Research.* 7(3):17-32, 1988.

Y. Nakamura, H. Hanafusa, and N. Ueno. A piezoelectric film sensor for robotic end-effectors. In A. Pugh, editor, *Robot sensors, Volume 2: Tactile and Non-Vision*, pages 247-57, IFS Publications/ Springer-Verlag, Berlin, 1986.

E. J. Nicolson and R. S. Fearing. The reliability of curvature estimates from linear elastic tactile sensors. *To appear in 1995 IEEE International Conference on Robotics and Automation*, Japan, 1995.

J. K. Salisbury. Interpreting contact geometries from force measurements. *Proceedings of the 1st International Symposium on Robotics Research.* Bretton Woods, NH, Sept. 1984.

J. K. Salisbury. Kinematic and force analysis of articulated hands. In M. T. Mason and J. K. Salisbury, editors, *Robot Hands and the Mechanics of Manipulation.* MIT Press, Cambridge, MA 1985.

P. Sikka, H. Zhang, and S. Sutphen. Tactile servo: control of touch-driven robot motion. *Experimental Robotics III: The Third International Symposium.* Springer-Verlag, Lecture Notes in Control and Information Sciences, vol. 200 pages 221-233. Kyoto, Oct. 28-30, 1993.

T. Tsujimura and T. Yabuta. Object detection by tactile sensing method employing force/torque information. *IEEE Transactions on Robotics and Automation*, 5(4):444-50, August 1989.

array sensor signal. The peak localization scheme is significantly different from the centroid schemes. This tells us that violating our initial assumption about single point contact affects the peak localization algorithm the most.

For the case of rotating a box shown in figures 10a and 10b, the contact location changes as the finger tip rolls against the box. Actual peak to peak object rotation is slightly less than 40 degrees since the fingers roll against the object, and this effect is not taken into consideration in the controller calculations. Because of slow manipulation speed and the absence of shear forces during rolling, both sensing schemes show about the same accuracy in tracking the contact location.

Careful examination of the peak localization scheme in figure 10a reveals discontinuities in the localization trace. Ideally, the finger and the box should form a uniform line contact, but during manipulation, the peak strain jumps positions within this line of contact due to edge effects and non uniform loading associated with manipulation. Since all the tactile elements were used for the peak detection algorithm, these effects reveal themselves as discontinuities in the trace.

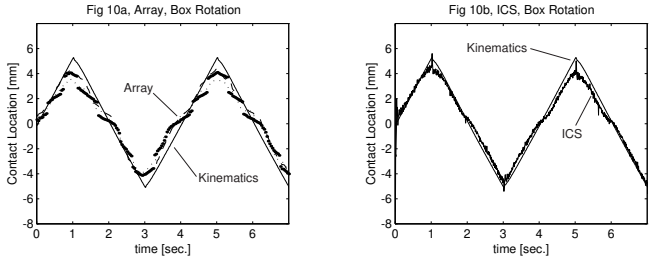

Figure 10. Contact localization for box rotation experiment. (a) Array sensor; (b) ICS. Solid line represent calculated results using robot kinematics.

5. Discussion

For many years, tactile sensing has promised to improve dexterity of robots. The goal of this paper is to examine fast, practical methods which can be implemented easily on real manipulators. From these calculations and experiments we can derive several important lessons. Both the tactile array and the ICS schemes were able to localize contact within a few millimeters in the presence of manipulation noise such as shear and inertial forces. Although the hardware for the ICS is much simpler, there are serious difficulties in the calibration procedure, especially with soft finger tips. When calibrating a force sensor for this application, it is important to precisely control the contact locations as well as the magnitudes and orientations of the applied point-load forces. However, a point load indents the rubber finger tip, making contact location imprecise and generating shear forces. This is a generic problem for all force sensors with compliant finger tips.

The ICS algorithm should be thresholded to obtain reliable contact location during initial contact. Before firm contact is established, the signal levels are on the order of the noise level so the localization errors are large. In addition, inertial forces can affect the ICS method, so rapid accelerations generated during manipulation should be minimized or ICS derived location should be ignored during that period. One way to reduce inertial forces is to use a smooth trajectory which minimizes accelerations. Another method involves minimizing the finger tip weight. Since the calibration is conducted on the finger tip surface, any forces generated on the surface, including object inertial forces, will be taken into consideration in the calculations. Therefore, only the inertial forces generated by the finger tip mass affect the localization scheme. This phenomena can be observed by the fact that despite an object weight ratio of 18:1 for the box to the pin, localization errors associated with the translation experiments remain essentially constant.

The tactile array sensor, on the other hand, is a more complex device. It requires a far greater effort to fabricate the sensor and the associated electronics. The calibration procedure required for the array sensor would have been similar, but using compressed air simplified the calibration procedure tremendously. In addition, the spatial characteristics of the sensor elements are uniform, so spatial calibration is not required. The lower mass associated with the array sensor makes it less susceptible to sudden accelerations for those elements not in contact with the object.

The three schemes for localizing contact provided interesting comparisons. The primary difference between the schemes seemed to be their sensitivity to shear forces, with the simple centroid scheme being most susceptible. For point contacts, the peak and thresholded algorithms worked well in rejecting shear induced strains. However, the centroid schemes performed better for larger contact areas. This suggests that the type of algorithm used should be tailored to the expected contact conditions.

Examination of the array sensor pressure distribution during box manipulation reveals that the pressure distribution is not uniform as expected. There are edge effects and shifting of peak locations. This creates some difficulty for the peak localization scheme which jumps from one peak to another in a discrete fashion. This suggests that for manipulating flat objects, a spherical tactile sensor or a softer rubber surface might provide more consistent information.

6. Conclusions

This paper presents calculations and measurements of localization errors in characteristic manipulation tasks using intrinsic contact sensing and tactile array sensing schemes. With the exception of ICS transients, experimental results show that the RMS localization error for all the sensing schemes are less than 1 mm. The ICS scheme, while potentially fast and accurate, requires a great deal of care in the calibration process, and it is affected by transient forces (e.g. initial contact, object accelerations) which can produce errors of several millimeters. Therefore, to effectively use ICS, finger tip mass should be minimized, contact forces should be thresholded before applying the algorithm, and either accelerations should be minimized or transients must be taken into account.

The tactile array sensor works well for contact localization. However, it is inherently slower than ICS and much more difficult to construct and integrate with the rest of the manipulator and controller. The tactile array sensor's sensitivity to shear loads was minimal and only noticeable at very sharp angles using a simple centroid scheme. For manipulation purposes, the shear load effects can be minimized

but it was repeated several times. The measured peak accelerations at the corners of the trajectory were between 80 and 130 cm/sec^2.

For figures 7a and 7b the actual trajectory of the contact location is a horizontal line at position 0 mm, and for figure 7c and 7d the actual trajectory is a horizontal line at -3mm. We observe that the random noise associated with ICS is larger in comparison to the tactile array sensor. There are two reasons for this. First, the random noise level of the force sensor was higher than the array sensor. Second, the finger tip mass acts along with the force sensor to mechanically amplify any vibrations and manipulator transmission noise.

Although the contact location does not change against the finger tip, localization spikes are seen every 0.5 seconds in figures 7b and 7d where the trajectory goes through a corner and inertial forces are generated. A clear correlation between object accelerations and localization ability for the ICS is shown by the periodicity of the trace corresponding to object accelerations. Figure 7a shows that the array sensor is immune to accelerations, but figure 7c shows that when the contact location is shifted approximately 3 mm, shear forces influence the centroid algorithm. Since the simple centroid algorithm uses all the tactile elements of the sensor, shear force generated deflections far from the contact location are included in the calculations, thus biasing the results.

Results from the pin rotation experiments are shown in figures 8a through 8d. In figures 8a and 8b, the pin is located at the center of the finger while for figures 8c and 8d, the location is shifted again by 3 mm. While holding a pin and rotating it, the contact location does not change against the finger tip, but the force vector changes along with the rotation angle. Since the contact location is fixed, the actual trajectory for these plots is also a horizontal line. Shear forces generated during the pin rotation experiment reduces the tactile array sensor's ability to localize contact since shear forces create normal strains. However, this localization error is only pronounced for the simple centroid scheme at very sharp angles as shown in figure 8c.

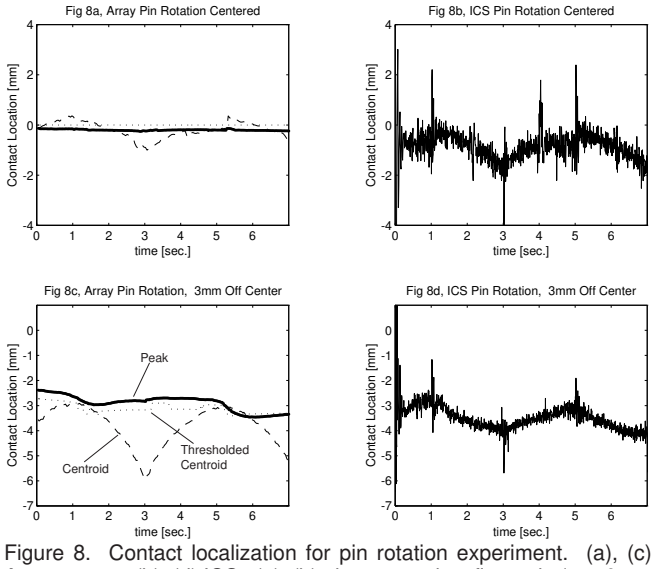

Figure 8. Contact localization for pin rotation experiment. (a), (c) Array sensor; (b), (d) ICS. (a), (b) pin centered on finger tip ($\theta = 0$, no shear forces); (c), (d) pin displaced 3 mm ($\theta = 0.19$ rad, shear force present).

Although the noise associated with the ICS signal hasn't increased, the localization trajectory is significantly different from the expected and the array sensor results. Theoretically, the ICS scheme should be insensitive to shear forces since it uses this information, but calibration difficulties result in errors, as seen by the "triangular wave" deviations from the actual location.

As seen in figures 8b and 8d, localization error spikes are observed for ICS due to rapid acceleration when the direction of rotation changes. Additional localization spikes are seen when $\theta = 0$ for figure 8b. Force transients can be generated when the object goes though $\psi = 0$ due to sign reversal of the shear force on the compliant rubber skin.

Table 1 compares the localization errors associated with each of the sensing schemes for the pin rotation and translation experiments. Since we are interested in larger systematic errors rather than random errors associated with sensor's signal to noise ratio, we observe the following. First, transient peak errors for ICS are several times larger than the array sensor. Second, shear forces introduced in the pin rotation experiment only affects the centroid algorithm of the tactile array sensor. This error, is most clearly seen during off centered pin rotation.

	Centroid	Threshold	Peak	ICS
Pin Translation Centered - RMS Error [mm]	0.05	0.10	0.09	0.18
Pin Translation Centered - Peak Error [mm]	0.12	0.17	0.23	1.10
Pin Rotation Off Center - RMS Error [mm]	0.78	0.18	0.25	0.34
Pin Rotation Off Center - Peak Error [mm]	2.94	0.40	0.52	2.42

Table 1. RMS and peak localization errors for the pin rotation and translation experiements without the initial contact transient errors.

4.3.2 Box Manipulation Experiments

For plots 9 and 10, the experiments involved translating and rotating a box, similar to the pin experiments. Contact locations calculated based on the kinematics of the robot and the object are plotted as a solid line for comparison purposes. This calculation requires a priori knowledge of object properties which would not be available in unstructured environments, but represents a reasonable approximation to the actual contact location.

The expected trace for the box translation experiment in figures 9a and 9b is a trapezoidal wave since the fingers roll mostly during the vertical traverse phase. Again, the ICS trace has more high frequency noise than the array sensor traces, even though the frequency content of the ICS data is mostly under 20 Hz, and thus comparable to the bandwidth of the

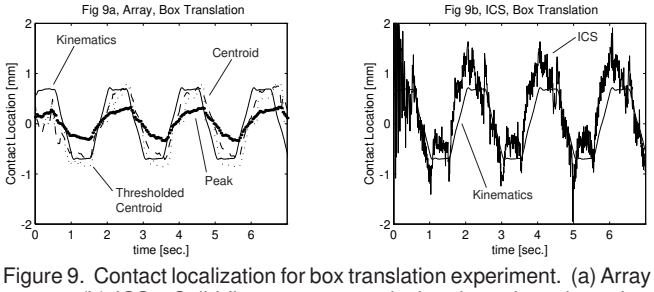

Figure 9. Contact localization for box translation experiment. (a) Array sensor; (b) ICS. Solid line represent calculated results using robot kinematics.

An error occurred while printing this page.
Error: **syntaxerror** Offending Command: **----nostringval----**
Suggestions:
PostScript interpreter did not understand the command. Try
proof print or moving some of the non-printing elements
off the page.

set t… …y and ICS localization
the … …ingers were positioned
worl… …manded a feedforward
arra… …ata acquisition started
15.7 … …orce of 3 N was used to
… …e object. Initial impact
4.2 I… … approximately 1N in
magnitude. This along with the zero contact force before contact explains the large localization error associated with the intrinsic contact sensing scheme at the instant of contact as shown in figure 6. The array sensor is insensitive to this contact transient.

To investigate contact localization during manipulation, two objects and two manipulation tasks were chosen. A 10 cm long pin with spherical 1.6 mm radius tip, and a 10 cm wide square box were used as the objects. The pin and the box weighed 4.2 and 77 grams respectively. The two manipulation tasks involved rotating the object ±20 degrees about the center of the object, and moving the object in a 2 cm by 2 cm square trajectory at a relatively high velocity of 4 cm/second.

These particular objects and tasks were selected to include many of the conditions that might be encountered in general dexterous manipulation tasks. In particular, the tasks generate significant shear forces and accelerations. When rotating the pin, the force angle with respect to the finger changes. This generates shear forces at the contact location which may reduce the localization ability of the array sensor. On the other hand, intrinsic contact sensing measures shear forces and uses this information to localize contact so variations in shear forces are taken into consideration. Since the object is a pin and the contact location remains essentially constant, the actual localization plot as a function of time should be a horizontal line. To measure the ability to track changes in contact location, the pin was replaced with a box having the same dimensions in length. As the object rotates, the finger tip rolls on the object and the expected trace for contact localization is approximately a triangular wave form as a function of time.

The next task of translating the object was designed to test the ICS scheme. At the corners of the square trajectory, the grasped object and the finger tips experience high accelerations, so the mass of the object and the finger tips will generate inertial forces to which the force sensor will respond. These forces will appear as interference on the force sensor signal, but the tactile array sensor, with its low mass and distributed sensing elements, should not respond. We wanted to observe the effects of these accelerational forces on the ICS algorithm and to verify that the array sensor is immune to them. When translating the box, the finger tip must roll slightly against the box to obtain the desired trajectory, while the expected localization trace for the pin is a horizontal line as a function of time.

4.3 Results

In figures 6 through 10, typical localization results for intrinsic contact sensing and the three localization schemes for the array sensor are plotted. For all the array sensor plots, the heavy solid dots are the peak localization algorithm, the dashed lines are the simple centroid algorithm, and the dotted lines are the thresholded centroid algorithm. The coordinate origin for contact localization is set at the location corresponding to $\theta = 0$ and the distance is along the circumference of the finger tip.

Figure 6. Comparison of transient responses of intrinsic and array sensing schemes. Large negative spike in ICS output is due to low force levels at initial contact.

4.3.1 Pin Manipulation Experiments
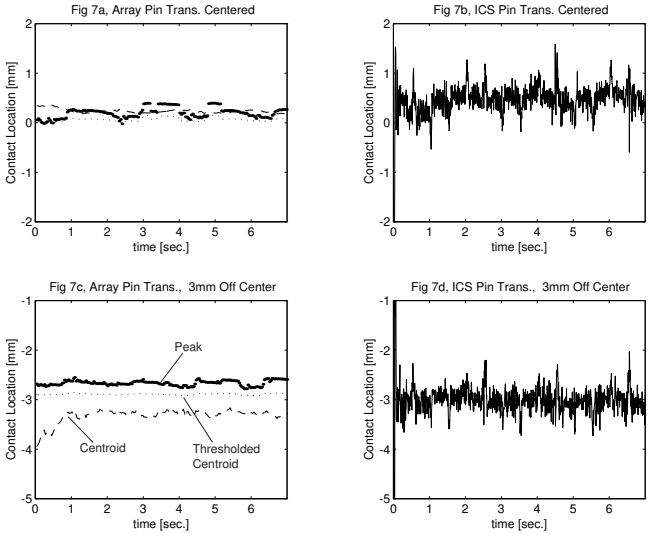
Results from translating the pin in a square trajectory are shown in figures 7a through 7d. In figures 7a and 7b, the pin is located at the center of the finger and shear forces were negligible, while for figures 7c and 7d, the contact location is shifted by approximately 3 mm and shear forces with respect to the surface normal were about 19% of normal forces. Since the object velocity was 4 cm/sec and the total length of the trajectory was 8 cm, the trajectory was completed in 2 seconds,